PHYSICAL REVIEW B, VOLUME 65, 075417

Local switching in epitaxial YH_x switchable mirrors

J. W. J. Kerssemakers, S. J. van der Molen, R. Günther, B. Dam, and R. Griessen
Division of Physics and Astronomy, Faculty of Sciences, Vrije Universiteit,
De Boelelaan 1081, NL-1081 HV, Amsterdam, The Netherlands
(Received 5 July 2001; published 1 February 2002)

All the essential switchable mirror properties of YH_x exhibit a strong hysteresis that is related to the structural β-dihydride to γ-trihydride phase transition. This structural transition in YH_x has so far been difficult to investigate since polycrystalline YH_x films are optically homogeneous on the length scale of visible light wavelengths. However, in *epitaxial* YH_x films the relation between *local* structural changes and *local* optical transmission can be investigated using *in situ* atomic force microscopy and optical microscopy, in hysteretic yttriumhydride mirrors exhibiting the earlier reported, domainwise pixel switching. We find widely varying local switching kinetics during the whole hydrogenation process. As a result, an epitaxial mirror forms essentially an ensemble of individual microcolumns, each of which can be in three regimes: (i) a single-phase regime of the β dihydride phase, where the optical transmission lowers with increasing hydrogen concentration, (ii) a layered two phase configuration in which the optical transmission rises with the fraction of high-concentration γ phase, and (iii) a single-γ-phase regime in which the transmission still increases significantly. The effect of a wide distribution of local properties on the global mirror properties are discussed within a simple model.

DOI: 10.1103/PhysRevB.65.075417 PACS number(s): 78.66.−w, 73.61.−r, 68.60.−p

I. INTRODUCTION

Switchable mirrors made of thin rare-earth (RE) metal hydride films change reversibly between a conductive reflective RH_3 and insulating transparent RH_3 state, during absorption or desorption of hydrogen. After the discovery of these switchable mirrors[1] in 1996, research was focused on their optical[2,3] and electronic[4–7] properties, which change over many orders of magnitude as the hydrogen concentration $x=[H]/[Re]$ is varied between 2 and 3. Later, it was realized that the *structural* properties of mirrors exhibit equally spectacular reversible effects. The best example is ''pixel switching,'' a large-scale discretization of both optical and structural switching occurring in *epitaxial* switchable YH_x mirrors.[8] During the first hydrogen exposure, the mirror surface self-organizes in a pattern of micrometer-sized domains, defined by a permanent triangular ridge network[9–11] as in Fig. 1(a). During the reversible loading (or unloading) between YH_2 and YH_3, each of the enclosed domains loads (unloads) homogeneously at an individual rate, thus implying a blocked lateral hydrogen transport[3] between adjacent domains. As a result of the relatively large size, switching can be observed optically in each triangular domain. Similarly, the structural transitions proceed via a dynamic pixel pattern of expanding (during H absorption) and contracting (during H desorption) domains. This effect is not observed optically in polycrystalline mirrors, probably because the domains are smaller than the wavelength of light.[2,12–14] Still, the global resistivity and optical transmission of a switching epitaxial film as shown in Fig. 1(b), are similar to those of a polycrystalline film. Thus the visibility makes the pixel switching phenomenon attractive as a natural model system for a question of great fundamental[4,6,7,14] and technological[15,16] relevance: namely, whether or not the optical transition takes place in a single hydride phase. This is in particular of great importance for the interpretation of the continuous metal-insulator transition in YH_x.[17] To answer this question, the relation between structural and optical switching should be investigated and understood on a microstructural level.

In this work, we present a quantitative study of the *local* relation between the optical transition (the ''switching'') and the structural phase transition as it occurs in epitaxial YH_x films. We show that a switching epitaxial mirror consists of an ensemble of domains with widely varying kinetics. Moreover, that each domain crosses three regimes during loading from YH_2 to YH_3: (i) a single-phase regime close to stoichometric YH_2, with the optical transmission lowering with increasing hydrogen concentration, (ii) a two-phase coexistence regime in which the transmission rises with the fraction of high-concentration γ phase present locally, and (iii) a single-phase (γ) regime in which still a significant optical change takes place. This implies that the metal-insulator transition occurs partly in a single γ phase whose optical properties are strongly H-concentration dependent.

II. EXPERIMENT

For a local measurement of the phase fraction, techniques such as *in situ* x-ray diffraction[13] are not suitable, as they only measure the average amount of each phase present. Instead, we exploit the uniaxial expansion that occurs during the fcc β ($YH_{1.9-2.1}$) to hexagonal γ ($YH_{3-\delta}$) reversible transition. For bulk YH_x, this expansion corresponds to 9.3%.[18] For simplicity, we use this value for our thin films, thus ignoring the effect of in-plane stresses on the out-of-plane expansion. In the case of an epitaxial film, this expansion is out of plane along the fcc [111] direction in the dihydride phase or, equivalently, the hexagonal [0001] direction in the trihydride phase. The corresponding height changes are proportional to the phase fraction underneath the atomic force microscopy (AFM) probe tip. They result in the pixel

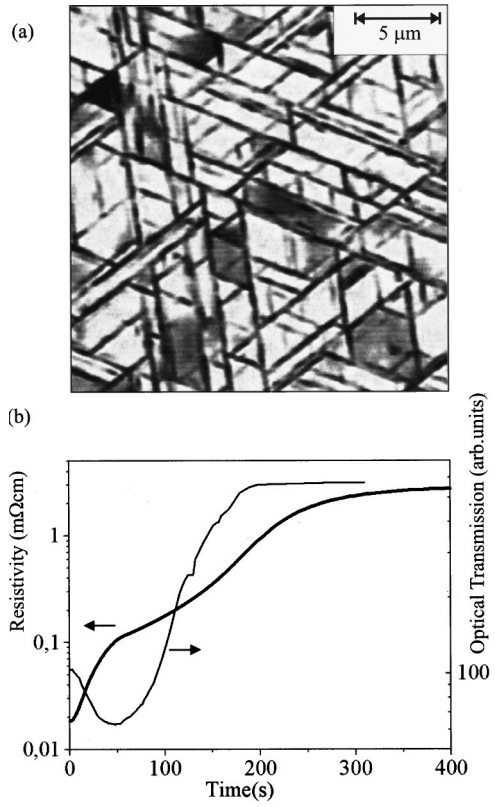

FIG. 1. (a) Blockwise switching. Optical transmission image of a 500-nm-thick epitaxial YH_x switchable mirror, capped by 3 nm of Pd. The film is in the process of unloading from the trihydride state. Visible is a triangular network of dark ridges along the 011 directions of the film, bounding domains. The domains are individually homogeneous, but have strongly varying optical transmissions relative to each other, implying that lateral hydrogen transport is blocked. A correlated, high-low pattern can be seen in the AFM topography of the surface (see also Fig. 3). (b) Global changes in resistivity (thick line) and optical transmission (thin line) of a similar, epitaxial, 300-nm-thick film loading from the dihydride to the trihydride state. Features are observed well known for both epitaxial and polycrystalline switchable mirrors.

switching[8] mentioned above, which can be perfectly monitored by *in situ* AFM.

To relate the phase fraction to other properties, we extended a standard atomic force microscope (Nanoscope III Multimode AFM) with a setup to measure simultaneously *local* topography, average optical transmission, and four-point electrical resistivity during controlled hydrogen loading (Fig. 2). For hydrogenation at room temperature, a standard ''fluid cell'' is used as gas cell through which a mixed air-hydrogen flow is led. Films are unloaded by flowing in air only. The optical transmission is measured using the built-in 600-nm laser of the AFM and a photodiode on the back of the sample. Although in the optical lever setup of the AFM the laser light is mainly reflected by the AFM cantilever, part of the light of the focused laser beam also illuminates the sample surface around the tip. As a result, a small, irradiated area is coupled to the scan movement. This is clearly seen in Figs. 2(b) and 2(c): A topography scan of a scratch made on an Y film produces an analogous image of

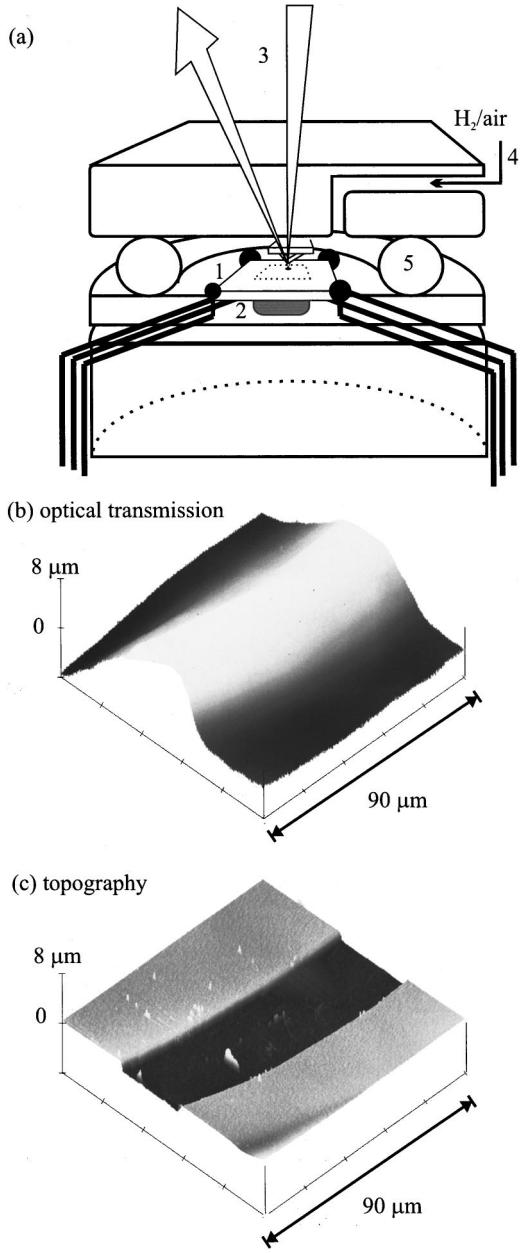

FIG. 2. (a) Schematic cross section of the *in situ* AFM setup. The resistivity of sample (1) is measured in a four-point arrangement (black dots). The average optical transmission is measured via a photodiode (2) collecting in coupled laser light (3) of the optical lever setup. Controlled (de)hydrogenation of the sample is accomplished by flowing a tunable H_2/gas mixture (4) through a cell sealed with an O ring (5). (b) Transmission image of a scratch through the film. By comparing with the sharp-edged topography image in (c), we derive an optical resolution of ~ 20 μm, indicating the semilocal character of the transmission measurement.

the local transmission, with a lateral resolution of approximately 20 μm. With respect to the discrete *optical* pattern (see Fig. 1) such a transmission measurement represents an average of the transmission over a large ($\sim$100) number of domains. However, as the illuminated area is of the same size as a typical AFM scan, the transmission obtained in this way is directly related to changes in the local topography observed simultaneously with the AFM.

The overall resistivity is measured in a four-point configuration[19] with contact pads fixed with silver paste on the outer rim of the sample. Additional measurements are carried out in an optical microscope in which four-point resistivity is also measured during hydrogenation to correlate AFM and optical microscope measurements.

Epitaxial yttrium films are prepared by ultrahigh-vacuum deposition (10^{-9} mbar) at substrate temperatures of 400–700 °C on (111) CaF_2. A thin Pd layer is put on top, as this is necessary to dissociate H_2 to atomic H during hydrogenation and to protect the Y film from oxidation. Prior to this Pd deposition, dry oxidation of the Y surface at 10^{-5} mbar for 25 min prevents Pd from diffusing into yttrium.[12,20] As described above, loading or unloading of such a film proceeds as blockwise pixel switching.[8] In Fig. 3(a), this is shown for a 500-nm YH_x/CaF_2 film capped by 3 nm of Pd, which is at some stage during unloading. As reported earlier,[8] a correlation between the optical and structural pattern exists, indicating the close interplay of the structural and optical switching. Here we establish the relation between local transmission and local phase fraction. To determine the phase fraction, we measure the local relative height of the surface. In doing so, we exclude the ridges, as they clearly divert in both topography as well as optical properties and do not represent undeformed material. For this particular film, the unloading rate was so slow that the time interval between the optical measurement and the AFM measurement could be ignored; this was checked by monitoring the optical transmission both before and after the AFM measurements.

Structurally speaking, the crystallographic orientation of the domains is still closely related to that of the as-deposited Y, contrary to the ridges.[21] Therefore, we only compare points on the domain surfaces, both in the optical and in the topographical micrographs. An example is shown in the inset in Fig. 3(c), where the optical profile of the bottom of a domain [indicated by the white line in Figs. 3(a) and 3(b)] closely follows the topography. Repeating this for a large number of points, we obtain a scatter plot of transmission versus relative height as shown in Fig. 3(c). The black dots correspond to the profile in Fig. 3(b). The maximum transmission of the mirror, measured previously after 2 days of loading at 1 bar of H_2, is indicated by the large open square.

The plot bears some intriguing implications. First, we note that the range of heights, expressed in % of the film thickness, again nicely covers the 10% expansion difference between the full β and full γ phase. This indicates that the left most points represent points on the surface which are fully β phase and the right most points correspond to fully hexagonal γ phase. Second, we note that the close match between height and transmission shown in the inset of Fig. 3(c) is only valid for intermediate height values, i.e., for those points on the surface where both phases are present underneath the AFM tip. For the γ phase, near 10% expansion in Fig. 3(c), we find a wide range of transmission values (indicated by the vertical bar). We conclude therefore that $\sim$50% of the optical switching takes place at an essentially constant height, i.e., in a single phase.

We stress that this plot was obtained essentially from *one* snapshot during unloading, represented by the AFM scan and its corresponding optical image: i.e., the plot depicts a mirror being in one *average* hydrogenation state. This average transmission value is indicated by the horizontal line in the plot. From this average measurement alone, one would conclude that the film entered the β-γ coexistence region. For a regular two-phase system this would mean that only one transmission value for the γ phase is present. On the contrary, we still observe nearly the full range of possible heights and transmissions. We conclude from these local measurements that an epitaxial mirror is by no means a standard, coexisting phase system, but that there is a wide spread in *local* switching rates.

Such a result could never have been obtained by comparing average values, e.g., via x-ray diffraction and *ex situ* transmission measurements. Moreover, the presence of a distribution of local transmission within the single γ phase implies that caution should be taken in the interpretation of global measurements.

During (re)hydrogenation of the mirror, each individual domain is exposed to a relative over-pressure of hydrogen and loads up to the trihydride state. The question is then how the distribution of hydrogenation states evolves with time. To answer this question we monitor the behavior of all pixels as a function of hydrogenation. For this, we perform in situ hydrogenation both in the optical microscope and in the AFM, while measuring at the same time average transmission and resistivity as reference parameters.

Figure 4 shows a typical example of a loading-unloading cycle of a 350-nm-thick YH_x/CaF_2 mirror, capped with 10 nm of Pd. In Fig. 4(a) the optical transmission changes as a function of resistivity, measured in the AFM, are shown while the sample is gradually loaded from YH_2 to YH_3 (upper curve). We observe a global minimum in optical transmission during loading, which is absent during unloading. The same hysteresis was reported in literature[13] for polycrystalline films, where the minimum was found to correspond to a concentration of $H/Y = 2.1$. The small oscillations in the transmission are caused by the scanning movement of the illuminated area. The relatively small amplitude justifies the use of this *semilocal* transmission as being representative for the *average* transmission of the sample. We stress that the true local, i.e., *imaging*, optical measurements are all performed independently in the optical microscope. In the AFM scans shown, the roman numbers correspond to the topography images in Fig. 4(b). We clearly observe changes in the image series, the domains rising one by one with respect to the ridges (which are inactive in this hydrogenation stage).[22]

We attribute the domain-by-domain surface rising in the series of AFM images in Fig. 4(b) to the β-γ transition in the vicinity of the AFM tip. This conclusion is drawn from an image-by-image tracking of *local* changes, to avoid AFM drift and overall sample bending disturbances. As the domains tend to switch at widely varying rates, most of the surface serves as a reference. This is shown in Fig. 5, where an initial, an intermediate, and an end profile are superimposed. From a larger number ($\sim$20) of profiles of consecutive AFM images during hydrogenation, we find a cumulative height change of 27 ± 5 nm, which is 8 ± 2% of the total

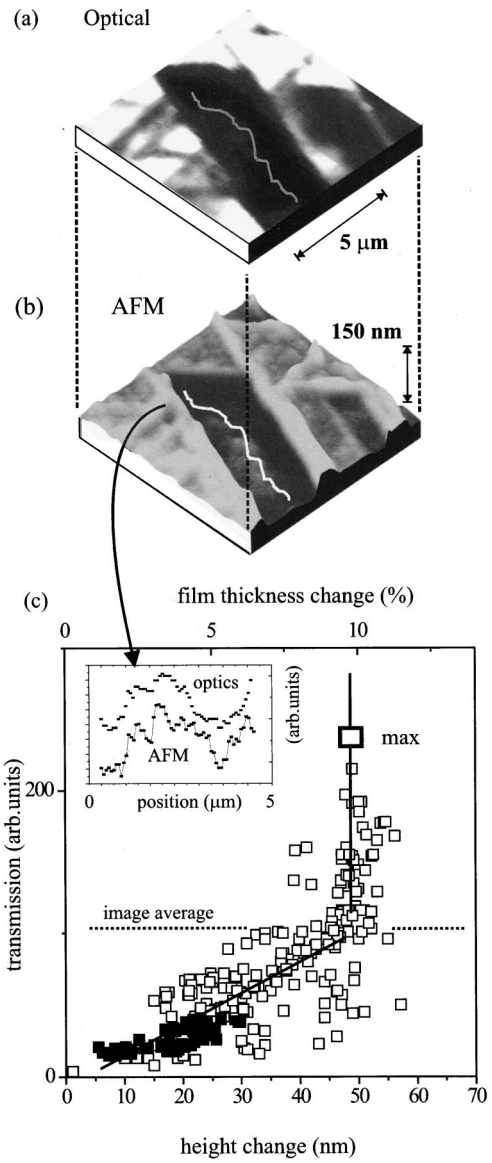

FIG. 3. Correlation between structural and optical switching. (a) Optical transmission and (b) AFM topography image of a 500-nm-thick epitaxial YH_x/CaF_2 film capped 3 nm of Pd, at a hydrogen concentration $x \sim 2.5$ during very slow unloading. A correlation between topography and transmission is clearly visible, for triangular and trapezoidal domains in various transmission and expansion states (surrounded by a network of ridges). (c) Optical transmission versus local height change. The small open and solid squares represent local points on the film surface (excluding the ridges), all taken in the same hydrogenation state of the YH_x film. The phase transition can be recognized from the ~50 nm height range at low transmissions, indicating the 10% lattice expansion during the phase transition. A continuous profile taken at the bottom of one domain reflects a close match between transparency and relative expansion in the coexistence regime (white profiles in inset, black solid squares in plot) In contrast, a large transmission range is visible for the maximum 10% expansion, indicating that the local hydrogen concentration in the hexagonal phase is strongly nonuniform. The maximum optical transmission of the mirror at 1 bar of H_2 pressure is indicated by the large open square. The horizontal line gives the average value of transmission for the imaged surface.

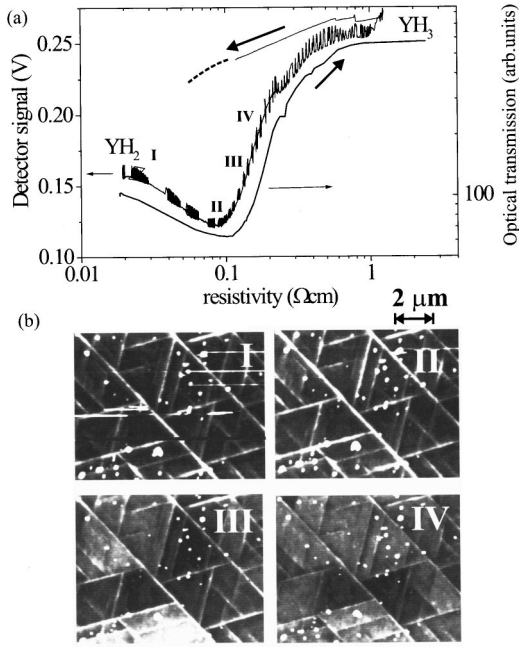

FIG. 4. (a) Optical transmission vs. resistivity (notched line) acquired during continuous hydrogen loading in the AFM of an epitaxial 350-nm-thick, Pd-capped YH_x/CaF_2 mirror. Notches in the curve occur whenever an AFM image is scanned. A similar curve (solid line) is shown for a subsequent loading cycle, which was performed in an optical microscope. Roman numbers correspond to AFM images in (b). The series of AFM images exhibits a selected area gradually switching from fcc-β to hexagonal γ-YH_x phase, visible as a relative expansion of the various domains. Domains are bound by ridges that block lateral hydrogen transport between domains and mechanically decouple them, resulting in independent behavior of neighboring domains.

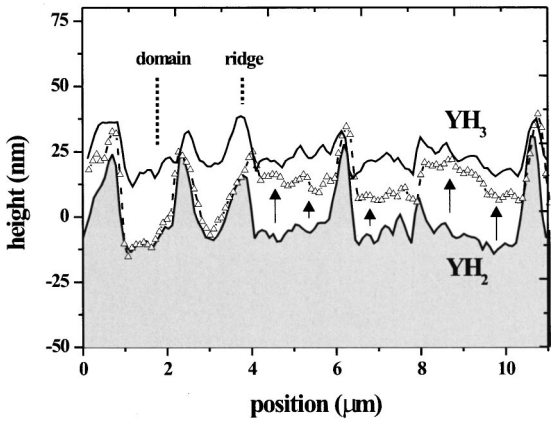

FIG. 5. Evolution of the surface profile of an epitaxial 350-nm-thick, Pd-capped YH_x/CaF_2 mirror during hydrogenation. The surface changes only locally, allowing for an absolute measurement of local changes between the dihydride surface (lower profile) and the trihydride surface (upper line). An intermediate profile (triangles) shows both rising as inactive segments. The total height increase corresponds to 8 ± 2 % of the total film thickness and reflects the fcc-β to hexagonal γ-YH_x structural transition, which involves a 9.3% *c*-axis expansion.

film thickness (350 nm). This value nicely corresponds to the expected 9.3% observed for the β-γ expansion[8,16] in bulk samples. This may be considered as an *a posteriori* confirmation of the relative reference method. Since the H-concentration dependence of the lattice expansion within the individual phases involved (β and γ) is small compared to the change resulting from the $\beta \rightarrow \gamma$ transition,[17] any measured relative height change reflects a local change of β-γ fractions.

A striking observation is that the transmission is *increasing* during the domain-by-domain β-γ transition, contrary to earlier reported *ex situ* measurements on polycrystalline films where the transmission minimum marked the end of the phase transition.[13] We note, however, that this earlier conclusion relied sensitively on the reproducibility of *absolute* values of resistivity, whereas the present setup has the great advantage that the structural *and* transmission changes are compared directly in the AFM. Moreover, recent *in situ* x-ray experiments on polycrystalline films are in agreement with the present results on epitaxial films.[23]

As mentioned before, we aim at linking the above structural dynamics to the simultaneously occurring optical changes. The *ex situ* method used in Fig. 3(c) is not well suited for this. We follow instead a statistical approach, making use of the reproducibility of the pixel switching, i.e., that during switching cycles of the mirror, the sequence in which domains switch remains the same.

After a full hydrogenation cycle (for example, the ninth) is completed in the AFM, the next cycle is performed in an Olympus BX60F5 optical microscope. Transmission versus resistivity (T vs ρ) plot of both loading cycles are shown in Fig. 4 (with use of the same contact pads). The fact that the T vs ρ plots from both microscopes have very similar features justifies the use of these plots as a reference.

To correlate the structural and optical dynamics, we convert the image series into height and transmission histograms, respectively. As an example, in Fig. 6(a) two height histograms are shown: one from the surface of a fully β-phase film (left peak) and one (right) taken from the same area, but at the end of the coexistence regime [cf. Fig. 4(b)-IV]. The simplicity of the surface structure (ridges and domains) allows us to associate the narrow peak with the domains and the tail (typically 20%–30%) with the ridges. The ridges do not switch structurally until all the domains have done so.[20] Their contribution leads to a shoulder in both histograms, which stays relatively immobile: for the right curve, this tail extends partly on the *left* side of the peak.

Figures 6(b) and 6(c) indicate the changes that occur in the topographical and transmission histograms during hydrogen loading. For each data point in the lower panels, a horizontal bar depicts the position of the peak value of the corresponding histogram [cf. Fig. 6(a)], while a vertical bar depicts the position of the full width at half maximum (FWHM). Both height and transmission histograms shift to higher transmission and height values during loading. The coexistence region lead to a relative increase in the distribution widths for both plots; see Figs. 6(b1) and 6(c1).

A number of interesting implications arise from a comparison of transmission and topography plots. (i) The onset

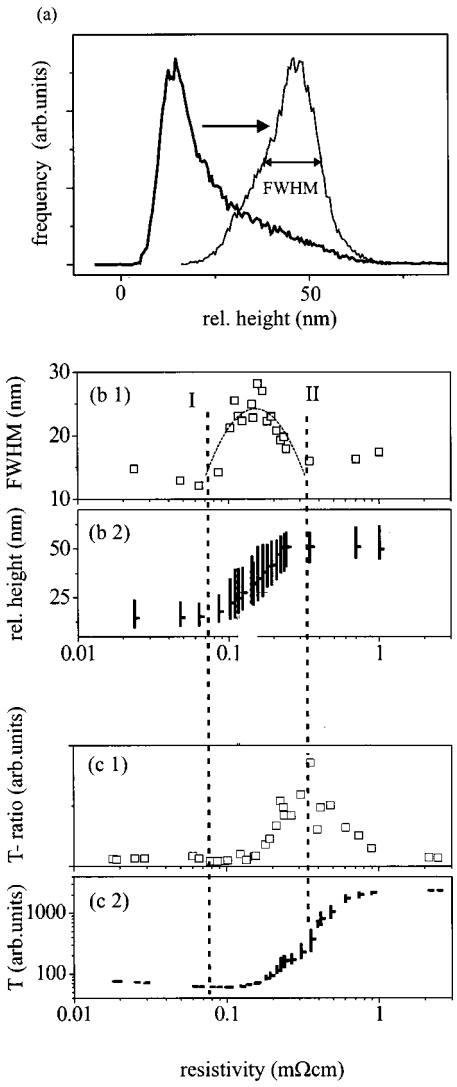

FIG. 6. Comparison of local and average measurements during loading. (a) Height histograms acquired from AFM topography scans. The contribution of domains (ridges) leads to the peaks (tails) both for the initial dihydride film (left curve) and the near-hexagonal phase film (right curve). Similar histograms can be acquired from transmission images. The peak values and FWHM values of both topography (b-I) and transmission (relative to the initial transmission) (c-I) are used to compare the local dynamic behavior in terms of phase coexistence (b-II) and optical transmission T (c-II). For the topography distribution the sharp increase in the FWHM marks the start (dashed curve I) of the β-γ coexistence region. A maximum spread in transmission (c-I) occurs near the end of the two-phase regime (dashed line II), indicating a large spread in both pixel kinetics and hexagonal γ-phase transmission.

of the structural coexistence region coincides with the minimal optical transmission (dashed line I). This indicates that the darkening of the film occurs in a single phase regime, contrary to the findings of Kooij *et al.*[13] (ii) The maximum spread in film transmission occurs near the end of the structural coexistence region (dashed line II). This agrees with the large spread in the optical transmission of the hexagonal phase found in the partially *unloaded* film (Fig. 3). Here we find also such a large spread for the *loading* process.

III. DISCUSSION

Summarizing, we find on a local scale that approximately 50% of the optical transmission occurs in the hexagonal γ phase, while the initial darkening of the film occurs fully in the fcc dihydride β phase. On a global scale, the film should be regarded as a collection of microscopic domain *pixels*, exhibiting a large spread in hydrogenation states at any moment.[7] The large switching rate difference between individual pixels governs the average phase fraction and transmission, indicating that great caution must be taken in interpreting switchable mirror properties only from average values. It is intriguing at this point to ask why polycrystalline and epitaxial films exhibit essentially the same overall optical transmission behavior during a hydrogen loading-unloading cycle, although these two types of films have very different microstructures.

In particular, during loading of polycrystalline films, Kooij *et al.*[13] observed that there is a well-defined exponential behavior during the rising of the transmission to its maximum value for $YH_{3-\delta}$. Such an exponential rise could be explained by a simple homogeneous two-layer system with a constant phase composition (i.e., height) on every point of the film surface, as schematized in Fig. 7(a). The results obtained in this work for epitaxial films imply that such a simple two-sheet model is far from reality (see Fig. 3). Instead, we observe a regime in which the domains clearly cover a large range of local phase fractions. Therefore we consider a model with a wide distribution of two-layered pixels [as in the left part of Fig. 3(c)]: we assume that the mirror consists of an ensemble of columnar domains, within which a bilayer of β and γ phases exists [see Fig. 7(b)].

An alternative geometry would be a ''fully columnar'' model, in which on each location the cross section of the film is either fully in the β phase or in the γ phase. However, we feel this is less appropriate to the actual situation for two arguments, based on the following experimental observations.

(i) The nature of the domain switching itself. The domains exhibit a relatively flat and optically homogeneous interior throughout the switching. This is clearly visible in Fig. 4(b), where individual domains rise gradually but stay flat. This is hard to combine with columnar switching (i.e., with vertical phase boundaries) as this would lead to strong height changes within each domain. From this, we argue that the left part of the plot in Fig. 3 represents a layerlike switching behavior.

(ii) Further, Grier *et al.*[10] (on HoH_x) and recently, Kooi *et al.*[21] (on YH_x) showed by high-resolution transmission electron microscopy (TEM) that both these epitaxial ReH_2 films (deposited on Nb-buffered Al_2O_3) consist of thin ($\sim$15–40 nm) horizontal lamellae of (111) fcc planes separated by planar defects running parallel to the substrate. In the case of YH_x these lamellae were present both before as after cycling to YH_3, suggesting that the fcc-β–hex-γ–fcc-β transitions are developing in a planar fashion, possibly incorporating Shockley-type partial dislocations.[21]

Further, in any layered system, in a first approximation it does not matter for optical properties or out-of-plane expansions how expanded layers are distributed over the film cross section: a domain divided only into two layers yields the same results as a domain with several (horizontal) phase boundaries, as long as the phase fraction is the same.

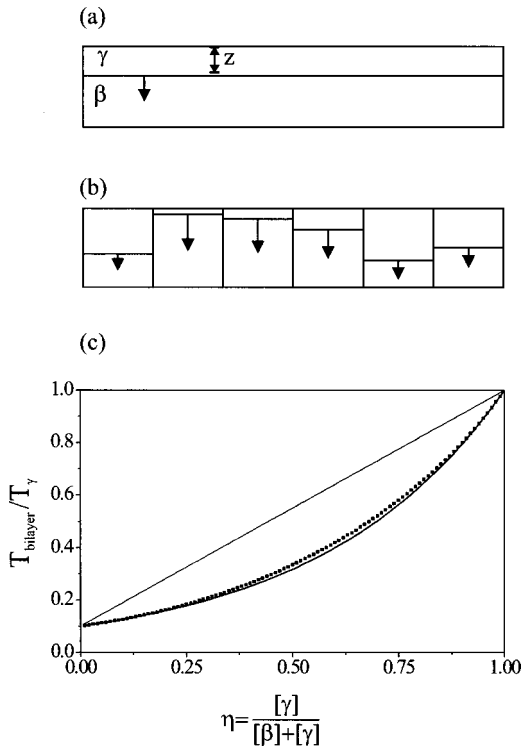

FIG. 7. Insensitivity of optical transmission to domain disorder. (a) Mirror in a coexistence phase state, with the β and γ phases stacked in a bilayer configuration. During switching, the phase front traverses vertically through the film, with each point having the same phase fraction present. The change in transmission follows exponential behavior as a function of phase fraction η [lower curve in (c)]. (b) Mirror with a distribution of local phase fraction, which has a maximum width $\Delta z = 2(1-z)z$ halfway the coexistence regime (see also Fig. 6). (c) The difference in average behavior of such a bilayer-domains model (dotted line) with the simple sheet model (lower curve) of (a) is only marginal. For comparison, the upper curve in (c) corresponds to a fully columnar phase distribution in which each domain consists either of β or γ phase.

The local fraction of β phase is taken as $(1-z)$ and that of γ phase is z. Thus $z=0$ corresponds to $x=2.1$ in YH_x and $z=1$ to $x=\sim 2.7$. A distribution $f(z)$ is defined in such a way that $f(z)dz$ is the fraction of bilayered pixels with a γ-phase fraction between z and $z+dz$. By definition,

$$\int f(z)dz = 1. \tag{1}$$

For simplicity, we assume that the phases are divided in only two layers covering the whole domain thickness (a multilayer structure would not alter the conclusions). Furthermore, we assume that the bilayer consists of two materials: fcc dihydride loaded up to $x=\mathrm{H/Y}=2.1$ (and thus at its lowest possible transmission) and the hexagonal γ phase when it just precipitated, i.e., at the lowest transmission for

this phase. In effect, we thus model the maximum contribution to the optical transmission that the domains in bilayer configuration could have. In such a bilayer configuration, the optical transmission T_{column} for one column is according to Lambert-Beer's law

$$T_{\text{column}}(x) = T_\gamma e^{A(z-1)}, \tag{2}$$

in which T_γ is the optical transmission of the dark γ phase and

$$A = d\left(\frac{1}{\lambda_\beta} - \frac{1}{\lambda_\gamma}\right), \tag{3}$$

where d is the thickness of the film and λ_β and λ_γ the frequency-dependent attenuation lengths for the β and γ phases. The average transmission $\langle T \rangle$ is given by

$$\langle T \rangle = \int T_\gamma e^{A(z-1)} f(z)\, dz. \tag{4}$$

For the present discussion, we choose for $f(z)$ a blocklike function with a width Δz and consequently a height of $1/\Delta z$ [Fig. 7(b)]. The average transmission is then

$$\langle T \rangle = T_\gamma e^{-A(1-\langle z \rangle)} \frac{\sinh(A\Delta z/2)}{A\Delta z/2}, \tag{5}$$

where $(1-\langle z \rangle)$ is the surface-averaged γ-phase fraction. The deviation from a uniform bilayer model is due to the sinh term within brackets. As long as $A\Delta z/2 < 1$, $\langle T \rangle$ reduces essentially to the homogeneous case. In the plot shown in Fig. 6(b-1), we observe that the *increase* in the distribution width can be attributed to the local presence of coexistent phases. The maximum increase is ~13 nm, which is of the order of 40% of the total height change (31 nm) when the domains load fully from the β to the γ phase. Thus the change in width Δx increase can well be described by

$$\Delta z = bz(1-z), \tag{6}$$

with $b \sim 2$. This in indicated by the dashed parabola in Fig. 6(b-1). Furthermore, from Fig. 3 we estimate $A \sim 2.3$. Thus $A\Delta z/2 < 0.6$. Combining Eqs. (5) and (6), we can compare the result with a simple two-layer system, as shown in Fig. 7(c). The deviation (which is greatest at $z = 0.5$) turns out to be completely negligible. For comparison a linear curve is added that depicts the change of the average transmission if, instead of layers, the film would switch in columns.

Thus we find that by the introduction of a *distribution* of bilayers instead of a single-averaged-bilayer model leads to a negligible deviation from simple exponential behavior. This explains why polycrystalline films behave like ''averaged'' epitaxial films in their optical properties. The presence of layered biphase structures leads thus to an exponential contribution in the transmission that is essentially independent of the actual distribution of these bilayers.

Thus we find that at almost any hydrogenation state of the mirror, the individual domains or pixels can be in one of three hydrogenation states: (i) single β phase, (ii) a layered β-γ structure, and (iii) a single γ phase in which the transmission may still vary considerably, as can be seen from Fig. 3. In the single γ phase, changes in hydrogen concentration lead to a rather large range in the optical transmission. Moreover, as can be seen from Fig. 3, this full range can still be present even when the average transmission indicates that the mirror is quite low in *average* hydrogen concentration.

Compared with the above simple bilayer model, a varying transmission for the single γ phase implies that a loading mirror brightens faster than can be accounted for by the change in phase fractions only. For the mirror as a whole, this means that phase fraction and average transmission cannot be simply related by only taking average values into account, as the contribution in transmission of the fraction of γ phase can vary significantly. Nevertheless, based on *local* measurements we show by simple modeling that the average transmission is surprisingly insensitive to the exact distribution of the phases present, provided that they are distributed in a layerlike fashion. This is of great advantage, as it implies that from average transmission measurements the minimal contribution of the single phase can be estimated by comparing the *increase* in transmission, with the *increase* in γ phase fraction (as can be measured by x-ray diffraction) without knowing the details in the distribution exactly. Recent measurements on polycrystalline mirrors support this possibility.[23]

IV. CONCLUSIONS

We conclude that, despite the large difference in local appearance, the average optical transmission of epitaxial and polycrystalline switchable mirrors changes similarly upon hydrogen loading. The visibility of the local distribution of phases in epitaxial mirrors made it possible to identify three typical states in which any point on the mirror can be in: (i) a single β phase, (ii) a layered β-γ structure, and (iii) a single γ phase in which the transmission may still vary considerably. The contribution of the latter can be extracted from the changes in the average transmission relative to the changes in average phase composition of the switching mirror, a result which preserves the value of averaged measurements on switchable mirrors. Nevertheless, in general these findings stress the need of local measurements in fundamental mirror research.

ACKNOWLEDGMENTS

This work was supported by the Stichting voor Fundamenteel Onderzoek der Materie (FOM), which is financed by N.W.O. We also acknowledge financial contribution of the European Commission through the TMR program (research network ''metal hydrides with switchable physical properties'').

[1] J. N. Huiberts, R. Griessen, J. H. Rector, R. J. Wijngaarden, J. P. Dekker, D. G. de Groot, and N. J. Koeman, Nature (London) **380**, 231 (1996).
[2] M. Kremers, N. J. Koeman, R. Griessen, P. H. L. Notten, R. Tolboom, P. J. Kelly, and P. A. Duine, Phys. Rev. B **57**, 4943 (1998).
[3] F. J. A. den Broeder, S. J. van der Molen, M. Kremers, J. N. Huiberts, D. G. Nagengast, A. T. M. van Gogh, W. H. Huisman, N. J. Koeman, B. Dam, J. H. Rector, S. Plota, M. Haaksma, R. M. N. Hanzen, R. M. Jungblut, P. A. Duine, and R. Griessen, Nature (London) **394**, 656 (1998).
[4] R. Eder, H. A. Pen, and G. A. Sawatzky, Phys. Rev. B **56**, 10 115 (1997).
[5] P. van Gelderen, P. A. Bobbert, P. J. Kelly, and G. Brocks, Phys. Rev. Lett. **85**, 2989 (2000).
[6] K. K. Ng, F. C. Zhang, V. I. Anisimov, and T. M. Rice, Phys. Rev. B **59**, 5398 (1999).
[7] P. J. Kelly, J. P. Dekker, and R. Stumpf, Phys. Rev. Lett. **78**, 1315 (1997).
[8] J. W. J. Kerssemakers, S. J. van der Molen, N. J. Koeman, R. Gunther, and R. Griessen, Nature (London) **406**, 489 (2000).
[9] D. G. Nagengast, J. W. J. Kerssemakers, A. T. M. van Gogh, B. Dam, and R. Griessen, Appl. Phys. Lett. **75**, 1724 (1999).
[10] E. J. Grier, O. Kolosov, A. K. Petford-Long, R. C. C. Ward, M. R. Wells, and B. Hjörvarsson, J. Phys. D **33**, 894 (2000).
[11] A. Pundt, M. Getzlaff, M. Bode, R. Kirchheim, and R. Wiesendanger, Phys. Rev. B **61**, 9964 (2000).
[12] S. J. van der Molen, J. W. J. Kerssemakers, J. H. Rector, N. J. Koeman, B. Dam, and R. Griessen, J. Appl. Phys. **86**, 6107 (1999).
[13] E. S. Kooij, A. T. M. van Gogh, D. G. Nagengast, N. J. Koeman, and R. Griessen, Phys. Rev. B **62**, 10 088 (2000).
[14] A. T. M. van Gogh, D. G. Nagengast, E. S. Kooij, N. J. Koeman, and R. Griessen, Phys. Rev. Lett. **85**, 2156 (2000).
[15] R. Armitage, M. Rubin, T. Richardson, N. O'Brien, and Yong Chen, Appl. Phys. Lett. **75**, 1863 (1999).
[16] P. van der Sluis, M. Ouwerkerk, and P. A. Duine, Appl. Phys. Lett. **70**, 3356 (1997).
[17] A. F. Th. Hoekstra, A. S. Roy, T. F. Rosenbaum, R. Griessen, R. J. Wijngaarden, and N. J. Koeman, Phys. Rev. Lett. **86**, 5349 (2001).
[18] P. Vajda, in *Handbook on the Physics and Chemistry of Rare Earths*, edited by K. A. Gschneider and L. Eyring (Elsevier, Amsterdam, 1995), Chap. 20, pp. 207–291.
[19] L. J. van der Pauw, Philips Res. Rep. **13**, 1 (1958).
[20] A. T. M. van Gogh, S. J. van der Molen, J. W. J. Kerssemakers, N. J. Koeman, and R. Griessen, Appl. Phys. Lett. **77**, 815 (2000).
[21] B. Kooi *et al.*, J. Appl. Phys. (to be published).
[22] J. W. J. Kerssemakers, S. J. van der Molen, R. Gunther, B. Dam, and R. Griessen, J. Alloys Compd. **330-332**, 342 (2002).
[23] A. Remhof, J. W. J. Kerssemakers, S. J. v. d. Molen, and R. Griessen, Phys. Rev. B (to be published).